### RESEARCH Open Access



# Dual-targeting CSF1R signaling attenuates neurotoxic myeloid activation and preserves photoreceptors in retinitis pigmentosa

Jiangmei Wu<sup>1,2</sup>, Jing Zhang<sup>1,2\*</sup> and Bin Lin<sup>1,2,3\*</sup>

### **Abstract**

Retinitis pigmentosa (RP), a group of inherited retinal diseases characterized by progressive photoreceptor degeneration, features prominent microglial activation and monocyte-derived macrophage infiltration. While colony-stimulating factor 1 receptor (CSF1R) shows diverse roles in regulating microglial survival and behaviors in various neurodegenerative diseases, its functional significance in RP pathogenesis remains unclear. In this study, we observed upregulated CSF1R signaling specifically within disease-associated myeloid cells in the rd10 mouse model of RP. Targeted intervention via intravitreal CSF1R neutralizing antibodies and systemic PLX5622 administration achieved reduced myeloid proliferation and pro-inflammatory cytokine production and greater photoreceptor survival. Notably, CSF1R potentiation using recombinant IL-34 or CSF1 exacerbated neuroinflammation and accelerated photoreceptor degeneration. Mechanistic investigations revealed that infiltrating monocyte depletion by clodronate liposomes significantly reduced macrophage infiltration and preserved visual function. Using CX3CR1<sup>CreERV+</sup>/R26<sup>(DTRV+</sup>/rd10 mouse model, we observed that diphtheria toxin-mediated microglia ablation preserved retinal function. Overall, our findings demonstrate the prominent role of CSF1R in neurotoxic myeloid activation in the context of RP. Our results provide preclinical proof-of-concept that dual targeting of retinal and peripheral CSF1R pathways may offer a mutation-agnostic therapeutic strategy for inherited retinal degenerations.

Keywords CSF1R, Proliferation, Neuroinflammation, Photoreceptor degeneration, Microglia, Macrophages

### \*Correspondence:

Jing Zhang

jing0114.zhang@connect.polyu.hk

Rin Lin

b.lin@polyu.edu.hk

<sup>1</sup>School of Optometry, The Hong Kong Polytechnic University, Kowloon, Hong Kong

<sup>2</sup>Centre for Eye and Vision Research (CEVR), 17W Hong Kong Science Park, Shatin, Hong Kong

<sup>3</sup>Research Centre for SHARP Vision (RCSV), The Hong Kong Polytechnic University, Kowloon, Hong Kong

### Introduction

Retinitis pigmentosa (RP), a genetically heterogenous group of inherited retinal disorders caused by mutations, progressively degenerates photoreceptors and ultimately leads to irreversible vision loss [1, 2]. Despite the identification of numerous pathogenic mutations, approximately 40% of RP patients remain genetically uncharacterized, underscoring an urgent need for developing mutation-independent therapeutic strategies [3–7]. Recent research indicates that neuroinflammation plays a pivotal role in driving RP progression [8–11]. Pharmacological and genetical interventions targeting pro-inflammatory responses demonstrate significant neuroprotection in both RP animal models and human trials [11, 12],



© The Author(s) 2025. **Open Access** This article is licensed under a Creative Commons Attribution-NonCommercial-NoDerivatives 4.0 International License, which permits any non-commercial use, sharing, distribution and reproduction in any medium or format, as long as you give appropriate credit to the original author(s) and the source, provide a link to the Creative Commons licence, and indicate if you modified the licensed material. You do not have permission under this licence to share adapted material derived from this article or parts of it. The images or other third party material in this article are included in the article's Creative Commons licence, unless indicated otherwise in a credit line to the material. If material is not included in the article's Creative Commons licence and your intended use is not permitted by statutory regulation or exceeds the permitted use, you will need to obtain permission directly from the copyright holder. To view a copy of this licence, visit http://creativecommons.org/licenses/by-nc-nd/4.0/.

Wu et al. Journal of Neuroinflammation (2025) 22:193 Page 2 of 17

establishing neuroinflammation as a key pathogenic contributor and a promising therapeutic target in RP.

The neuropathology of RP involves coordinated activation of both resident microglia and infiltrating monocytederived macrophages, forming a pathological network driving photoreceptor degeneration [13, 14]. During RP progression, activated myeloid cells undergo characteristic morphological transformation from a ramified state to an amoeboid phagocytic phenotype, accompanied by increased phagocytic capacity and cytokine production, such as interleukin 1 beta (IL-1β), IL-6, and tumor necrosis alpha (TNF- $\alpha$ ) [9, 15], which subsequently not only stimulate resident microglia proliferation but also recruit circulating macrophages [9, 15–17]. The resultant expansion of myeloid cells exacerbates cytokine cascades, ultimately leading to neurotoxicity on photoreceptors [18]. While our previous work identified CX3CR1, COX-1 and TAK1 as modulators of microglial dynamics [8, 10, 19], emerging evidence reveals functional disparities of resident microglia and infiltrated macrophages in retinal degenerative diseases [9, 13, 20]. This cellular heterogeneity underscores an essential necessity for precise characterization of distinct myeloid subpopulations to dissect their individual contributions to RP pathogenesis.

Colony-stimulating factor 1 receptor (CSF1R), predominantly expressed on microglia and tissue macrophages, mediates survival and proliferation through binding to its ligands CSF1 and IL-34 [21, 22]. In neurodegenerative diseases, such as Alzheimer's disease, Parkinson's disease, and amyotrophic lateral sclerosis, CSF1R overexpression correlates with microglial activation, while its pharmacological inhibition demonstrates beneficial neuroprotective effects across multiple models [23]. Mechanistic studies show that CSF1R blockage suppresses pathogenic microglia activation via downregulation of lineage-determining transcription factors C/EBPα and PU.1, effectively controlling microglial proliferation [24, 25]. Despite these advances in central nervous system (CNS) diseases [23, 26, 27], the therapeutic potential of CSF1R modulation on the dual activation of resident microglia and infiltrating macrophages and photoreceptor degeneration in RP remains unexplored.

In the present study, we used rd10 mouse model of RP to perform spatiotemporal analysis of CSF1R signaling dynamics during photoreceptor degeneration, characterize CSF1R-mediated regulation of myeloid proliferation, and decipher relative contributions of microglial versus macrophage populations to RP pathology. Through different combinatorial approaches including intravitreal CSF1R neutralizing antibody, systemic PLX5622 administration and transgenic depletion mouse models, we observe that CSF1R serves as a critical regulator of neurotoxic myeloid activation. Notably, we demonstrate that both resident microglia and infiltrating macrophages

contribute to photoreceptor degeneration through cooperative mechanisms. Our results suggest targeting CSF1R as a combinatorial mutation-agnostic therapeutic strategy for RP.

### **Materials and methods**

### **Animals**

C57BL/6J mice (JAX:000664), rd10 mice (JAX:004297), CX3CR1<sup>CreER/CreER</sup> mice (JAX: 021160), CX3CR1<sup>GFP/GFP</sup> mice (JAX:005582), R26<sup>iDTR/iDTR</sup> mice (JAX:007900) were obtained from Jackson Laboratory. Rd10 mice were backcrossed with CX3CR1GFP/GFP mice to generate CX3CR1<sup>GFP/+</sup>/rd10 mice for use. CX3CR1<sup>CreER/CreER</sup> and  $R26^{iDTR/iDTR}\mbox{ mice}$  were backcrossed with rd10 mice to generate CX3CR1<sup>CreER/+</sup>/R26<sup>iDTR/+</sup>/rd10 mice for use. The genotypes were confirmed by PCR using primers listed in Table S1. For each independent experiment, age- and sex-matched mice were randomly assigned to different experimental groups. All experimental procedures were approved by the Animal Subjects Ethics Sub-committee (ASESC) of Hong Kong Polytechnic University and conducted in accordance with the Association for Research in Vision and Ophthalmology (ARVO) statement for the use of animals. All mice were housed in the Centralized Animal Facilities (CAF) of the Hong Kong Polytechnic University under a 12-hour light/ dark cycle with water and food ad libitum.

### **Drug administration**

To locally block CSF1R signaling, age- and sex-matched rd10 mice received an intravitreal injection of a CSF1R neutralizing antibody (1 µg; Ultra-LEAF™ Purified antimouse CD115, Clone AFS98, #135539, Biolegend) or an isotype control antibody (1 µg; Rat IgG) in the right eye at P16 with a dosage reported in previous study [28]. For intravitreal injection procedure, mice were anaesthetized via intraperitoneal injection of ketamine (50 mg/ kg) and xylazine (10 mg/kg), and pupils were dilated with 1% Tropicamide (Alcon) for 5 min. Topical analgesia was provided with 0.5% proparacaine hydrochloride (Provain-POS, URSAPHARM) prior to injection. The antibodies were delivered into the vitreous cavity using a 32G needle fitted to Hamilton syringe, with 0.5 µl injected at both the superior and inferior quadrants, just posterior to the limbus of the eye. Immediately following the injection, a topical hydrogel (Viscotears) was applied to the ocular surface to prevent corneal dehydration and minimize leakage from the vitreous cavity.

To systemically inhibit CSF1R signaling, rd10 mice received daily oral gavage of PLX5622 (#28927, Cayman) from P10 until the day of tissue collection [29]. PLX5622 was prepared by first dissolving 100 mg of compound in 100  $\mu$ l of DMSO, followed by dilution in 9.9 ml of corn oil to achieve a final concentration of 10 mg/ml. The

Wu et al. Journal of Neuroinflammation (2025) 22:193 Page 3 of 17

suspension was mixed thoroughly to ensure uniform distribution. Mice were weighed prior to each administration, and PLX5622 was delivered via oral gavage using a ball-tipped gavage needle at a dose of 90 mg/kg, as reported in previous study [30]. Control rd10 mice received the same volume of corn oil (containing 1% DMSO) without PLX5622, following the same administration schedule.

To induce CSF1R activation, rd10 mice received intravitreal injections of recombinant murine CSF1 (#M9170, Merck Chemicals), recombinant murine IL-34 (#5195-ML-010, R&D Systems), or PBS (vehicle control) in the right eye at P18. For solution preparation, 10  $\mu$ g of recombinant murine CSF1 or IL-34 was dissolved in 10  $\mu$ l of PBS to obtain a final concentration of 1  $\mu$ g/ $\mu$ l. Age- and sex-matched rd10 mice were intravitreally injected with 1  $\mu$ l of the prepared solution, following the same injection procedure as described above. Control rd10 mice received an equivalent volume of PBS, administered on the same schedule.

To deplete circulating monocytes, CX3CR1<sup>GFP/+</sup>/rd10 mice were given daily intraperitoneal injection of PBS-loaded or clodronate-loaded liposomes (C005, Liposoma) from P15 until tissue collection in a dosage of 50 mg/kg as suggested by supplier.

deplete resident microglia, CX3CR1<sup>CreER/+</sup>/  $R26^{iDTR/+}/rd10$  mice first received daily intragastric injection of tamoxifen (TAM, T5648, Sigma) from P1 to P4. TAM was dissolved in corn oil at a final concentration of 5 mg/ml by incubating at 37 °C overnight, protected from light. Prior to injection, 50 µg of TAM per pup was loaded into a syringe. Neonatal pups were gently restrained, and the location of the milk spot was identified to guide proper needle placement. The injection needle was inserted perpendicular to the abdominal skin, to a depth of approximately 2–5 mm, ensuring entry into the stomach. A volume of 10 µl of the TAM solution was slowly injected, after which the needle was carefully withdrawn. Pups were immediately returned to a warming pad and then to the home cage. To induce microglial depletion, mice received daily intraperitoneal injections of diphtheria toxin (DT, D0564, Sigma) from P17 to P19. DT was dissolved in sterile PBS at a final concentration of 1 ng/μl, and a dose of 20 μg/kg body weight was administered once daily. Mice received no TAM and DT serve as control.

### Immunostaining and confocal imaging

Mice were deeply anesthetized via intraperitoneal injection of ketamine (50 mg/kg) and xylazine (10 mg/kg) and subsequently euthanized by cervical dislocation. After marking a reference point denoting the superior pole, the eyes were enucleated and immersed in 4% paraformaldehyde (PFA) in PBS for one hour. The spleen tissues were

fixed in 4% PFA for 12 h. Retinas and spleen tissues were serially sectioned at a thickness of 14  $\mu$ m using a cryostat.

Whole-mounted retinas and tissue sections were incubated with blocking buffer (3% normal donkey serum, 1% bovine serum albumin, and 0.1% Triton X-100 in PBS) for one hour. Primary antibodies, including rabbit anti-Iba1 (1:500-1:1000, 019-10741, Wako), goat anti-Iba1 (1:500, ab5076, Wako), rabbit anti-CD44 (1:100, Millipore, MABF580), rabbit anti-GFP (1:500, A11122, Invitrogen), rabbit anti-Ki67 (SP6) (1:100, MA5-14520, Thermo Fisher), rabbit anti-CSF1R (1:400, 43390 S, CST), and rabbit anti-F4/80 (1:200, 70076 S, CST), were diluted in blocking buffer and incubated overnight to 3 days at 4 °C. After washing with PBS, secondary antibodies, including donkey anti-rabbit Alexa Fluor 488 (1:500, A21206, Invitrogen), donkey anti-goat Alexa Fluor 488 (1:500, A11055, Invitrogen), and donkey anti-rabbit 594 (1:500, A21207, Invitrogen), were applied to sections or whole-mount retinas at room temperature for 2-4 h. Nuclei were counterstained with DAPI (1:500, 1%, D8417, Sigma). After washing with PBS, sections and whole-mount retinas were mounted with Vectashield mounting medium (Vector Laboratories). Confocal images were acquired using a Zeiss LSM 800 upright confocal microscope (Carl Zeiss). Images were captured in the central region of the superior retina, approximately 200 µm from the optic nerve head, where outer nuclear layer (ONL) thickness, cell proliferation and apoptosis, and myeloid activation were subsequently measured.

### Terminal deoxynucleotidyl transferase dUTP Nick end labeling (TUNEL) assay

TUNEL assay was conducted with the In Situ Cell Death Detection Kit, TMR red (#12156792910, Roche), as per the manufacturer's instructions. Subsequently, the immunofluorescent staining was performed as described above.

### **EdU cell proliferation assay**

The mice received intraperitoneal injection of EdU (HY-118411, MCE) four times at a dosage of 50 mg/kg body weight, with a two-hour interval between each injection. Retina samples were harvested two hours after the final EdU injection. EdU labeling was visualized using the Click-iT™ EdU Cell Proliferation Kit for Imaging with Alexa Fluor™ 488 dye (C10337, Thermofisher), following the manufacturer's protocol. Subsequently, the immunofluorescent staining was performed as described above.

### **Evans blue assay**

CX3CR1<sup>GFP/+</sup>/rd10 mice received intraperitoneal injection of 0.2 ml of 2% Evans blue (E2129, Sigma). Six hours post-injection, the mice were perfused with 0.9% saline to clear the circulation before collection of brain and retina

Wu et al. Journal of Neuroinflammation (2025) 22:193 Page 4 of 17

tissues. The tissues were homogenized and incubated with formamide (1 g tissue in 10 ml formamide, Sigma) at  $55\,^{\circ}$ C for 24 h to extract the Evans blue dye. The resulting formamide-Evans blue mixture was centrifuged, and the absorbance of the supernatant was measured at 610 nm using a plate reader to quantify the dye, indicating barrier integrity.

### **qPCR**

Total RNA was isolated from individual retinas using Trizol reagent (#15596026, Thermo Fisher). Reverse transcription (RT) was performed using 1  $\mu g$  of RNA with High-Capacity cDNA Reverse Transcription Kit (Thermo Fisher). Quantitative PCR (qPCR) was performed using TB Green Premix Ex Taq (Tli RNase H Plus) (TaKaRa) on a QuantStudio 7 Flex Real-Time PCR System (Applied Biosystems) or a QuantStudio 5 Flex Real-Time PCR System (Applied Biosystems). Relative mRNA levels were determined using the  $2^{-\Delta\Delta Ct}$  method with GAPDH as the control. Primer sequences were listed in Table S1.

### Electroretinogram (ERG) analysis

Mice were dark-adapted overnight and anesthetized with a mixture of ketamine (50 mg/kg) and xylazine (10 mg/kg). Pupils were dilated with 1% mydriacyl (Alcon) 5 min before the experiment, and the cornea was coated with 3% hydroxypropyl cellulose lubricating gel solution (Alcon). ERG recordings were performed using the Celeris ERG System (Diagnosys, USA). Scotopic ERGs were recorded with increasing light intensities (0.01, 0.1, 1, and 3 cd.s/m²) to assess rod-mediated responses. Photopic ERGs were recorded after 10 min of light adaptation at a background light intensity of 30 cd/m², with light intensities of 3 and 10 cd.s/m² to assess cone-mediated responses. A- and b-wave amplitudes were analyzed using Celeris ERG software.

### Statistical analyses

Statistical analyses were performed using GraphPad Prism 10 software. For intravitreal treatments, only the right eye received experimental or control injections, while the left eye remained untreated. The right eye was used for ERG analysis, followed by qPCR or histological assessment. Similarly, for systemic treatments (intraperitoneal or oral), only the right eye was collected for analysis. As only one eye per animal was treated and analyzed, all samples were treated as independent. Accordingly, statistical analysis was performed using two-tailed unpaired Student's t-tests or one-way ANOVA with Tukey's post hoc test. P < 0.05 was considered statistically significant. Data are presented as mean ± standard deviation (SD). The detailed p-values, effect sizes, and confidence intervals for each figure and comparison are provided in supplementary file 3. Experiments were blinded to the genotype of the animal as well as the treatment of the animal.

### **Results**

### CSF1R signaling upregulation coincides with myeloid cell proliferation in rd10 mice

To investigate CSF1R signaling in RP, we used rd10 mice, a well-established mouse model of RP that carries a PDE6β mutation [11, 31]. We assessed CSF1R expression through double immunostaining of CSF1R with Iba1, a marker labels both microglia and macrophages. We focused on P16, P19, and P22, representing the onset to the peak of microglial activation [8]. From P16 onward, rd10 mice exhibited a significant increase in the number of Iba1+ cells compared to age-matched C57BL/6J mice (Fig. 1A and B), indicating myeloid cell expansion during degeneration. We identified CSF1R exclusively in Iba1+ cells and observed an increased percentage of CSF1R<sup>+</sup> cells in P22 rd10 mice compared to age-matched C57BL/6J mice (Fig. 1A and B). Additionally, stronger CSF1R immunoreactivity was observed in Iba1+ cells infiltrating from the outer plexiform layer (OPL) to the outer nuclear layer (ONL) in P22 rd10 mice (Fig. 1A), suggesting CSF1R upregulation in myeloid cells actively involved in degeneration. We further examined CSF1R signaling dynamics by qPCR. Consistent with immunofluorescent findings, we observed increased gene expression of CSF1R and its ligand CSF1 in rd10 retinas at P19 and P22 compared to age-matched C57BL/6J retinas (Fig. 1C). IL-34, another ligand for CSF1R, was upregulated at P19 but downregulated at P22 in rd10 retinas compared to age-matched C57BL/6J retinas (Fig. 1C). PU.1 and C/EBPα, downstream transcription factors of CSF1R signaling, were also upregulated in rd10 retinas compared to age-matched C57BL/6J retinas (Fig. 1C).

Since CSF1R signaling is essential for microglial proliferation in CNS neurodegenerative conditions [24], we further analyzed the expression of Ki67, a proliferation marker, in rd10 mice. Retina flat mount showed that Ki67 were nearly undetectable in Iba1<sup>+</sup> cells at P16 in both rd10 and C57BL/6J mice. However, by P19 and P22, approximately 40% and 60% of Iba1<sup>+</sup> cells expressed Ki67 in rd10 retinas, respectively (Fig. 1D and E). This indicates a significant increase in myeloid cell proliferation during degeneration, which coincides with the activation of CSF1R signaling.

### CSF1R inhibition attenuates neurotoxic activation of myeloid cells in rd10 mice

To study the role of CSF1R in myeloid cell activation, we inhibited CSF1R via intravitreal injection of a neutralizing antibody (anti-CSF1R) in rd10 mice at P16, prior to the onset of robust proliferation. Control rd10 mice received an isotype control antibody. Following

Wu et al. Journal of Neuroinflammation (2025) 22:193 Page 5 of 17

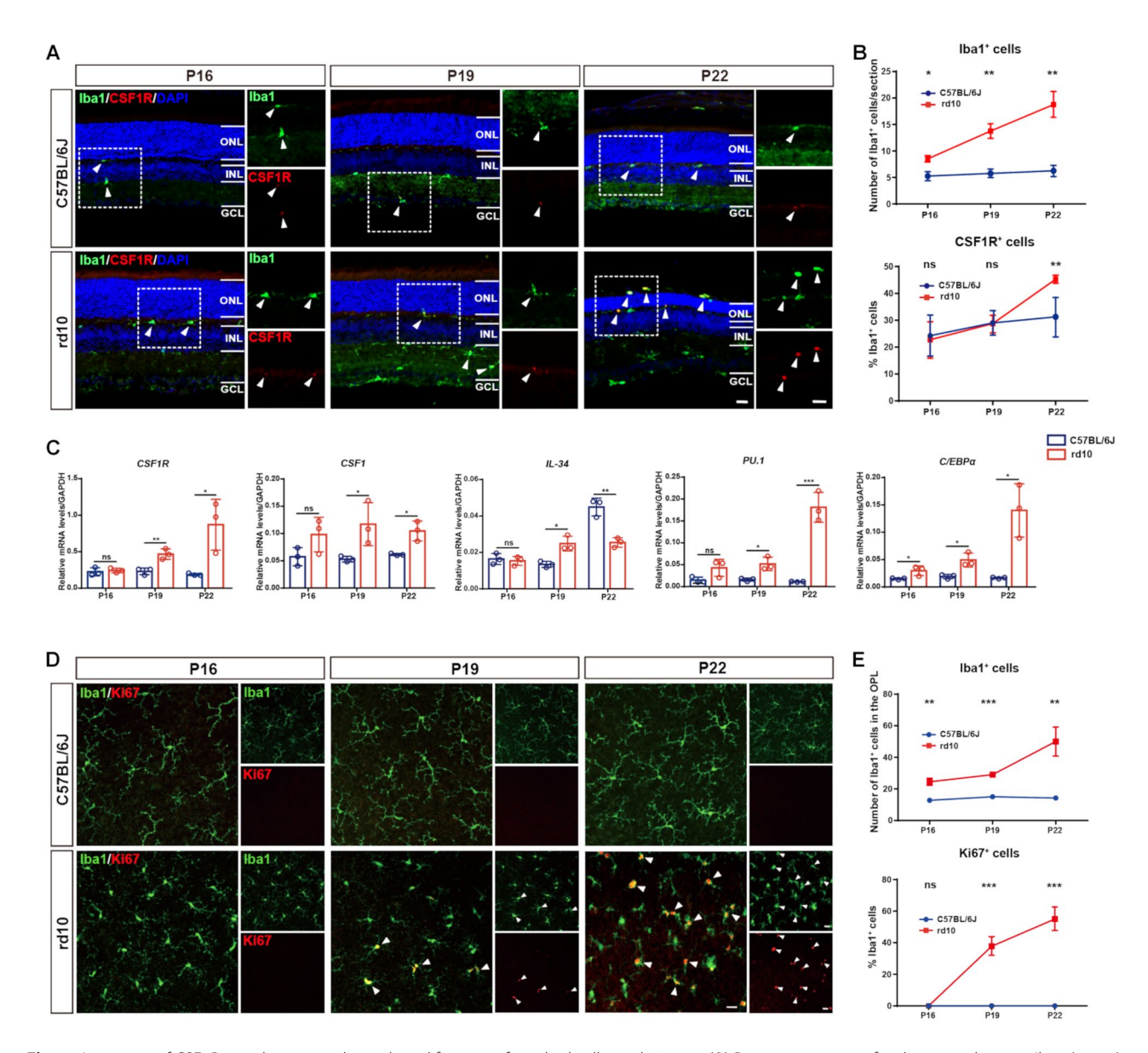


**Fig. 1** Activation of CSF1R signaling coincides with proliferation of myeloid cells in rd10 mice. (**A**) Representative confocal images showing lba1 (green) and CSF1R (red) on the retinal sections of P16, P19, and P22 rd10 and C57BL/6J mice (central region of superior retina, approximately 200 μm away from the optic nerve head). Cell nuclei are stained with DAPI (blue). White arrows indicate CSF1R<sup>+</sup> lba1<sup>+</sup> cells. ONL: outer nuclear layer, INL: inner nuclear layer, GCL: ganglion cell layer. Scale bar, 20 μm. (**B**) Quantification of lba1<sup>+</sup> cells (n=3 mice/group, C57BL/6J versus rd10, P16, p=0.0229; P19, p=0.0026; P22, p=0.0036). Quantification of the percentage of CSF1R<sup>+</sup> cells in lba1<sup>+</sup> cells (n=3 mice/group, C57BL/6J versus rd10, P16, p=0.7784; P19, p=0.9313; P22, p=0.009). (**C**) qPCR analysis of CSF1R signaling gene expression in rd10 and C57BL/6J retinas at P16, P19, and P22. (n=3 mice/group, CSF1R, P16, p=0.6426; P19, p=0.0085; P22, p=0.00275. CSF1, P16, p=0.1204; P19, p=0.0492; P22, p=0.0148. IL-34, P16, p=0.6661; P19, p=0.0109; P22, p=0.0036. PU.1, P16, p=0.0773; P19, p=0.0165; P22, p=0.001. C/EBPα, P16, p=0.0452; P19, p=0.0169; P22, p=0.0119). (**D**) Representative confocal images showing lba1 (green) and Ki67 (red) on the retinal flat mounts of rd10 and C57BL/6J mice. The images were stacked images of myeloid cells located in the outer plexiform layer (OPL). White arrowheads indicate Ki67<sup>+</sup>lba1<sup>+</sup> cells. Scale bar, 20 μm. (**E**) Quantification of lba1<sup>+</sup> cells (n=3 mice/group, C57BL/6J versus rd10, P16, p=0.0021; P19, p<0.0001; P22, p=0.0081). Quantification of the percentage of Ki67<sup>+</sup> cells in lba1<sup>+</sup> cells (n=3 mice/group, C57BL/6J versus rd10, P16, p=0.0021; P19, p<0.0001; P22, p<0.0001). Data are presented as mean ± SD and analyzed using unpaired Student's t-test for each time point (**B**, **C**, **E**). \*p<0.005, \*\*p<0.001, \*\*p<0.001, \*\*p<0.0001, \*\*p<0.0001, \*\*p<0.0001, \*\*p<0.0001, \*\*p<0.0001, \*\*p<0.0001, \*\*p<0.0

anti-CSF1R treatment, we observed less Iba1<sup>+</sup> cells (~50% reduction) and almost absence of Ki67<sup>+</sup> cells in rd10 retinas (Fig. 2A and B). Moreover, EdU incorporation demonstrated almost absence versus 30% of EdU<sup>+</sup> cells among myeloid cells after anti-CSF1R versus isotype

control treatment in rd10 mice (Fig. 2C and D), providing strong evidence of suppressed myeloid cell proliferation after CSF1R inhibition. Given the crucial role of CSF1R in microglia survival [21], we conducted TUNEL assay to determine whether increased apoptosis also contributes

Wu et al. Journal of Neuroinflammation (2025) 22:193 Page 6 of 17

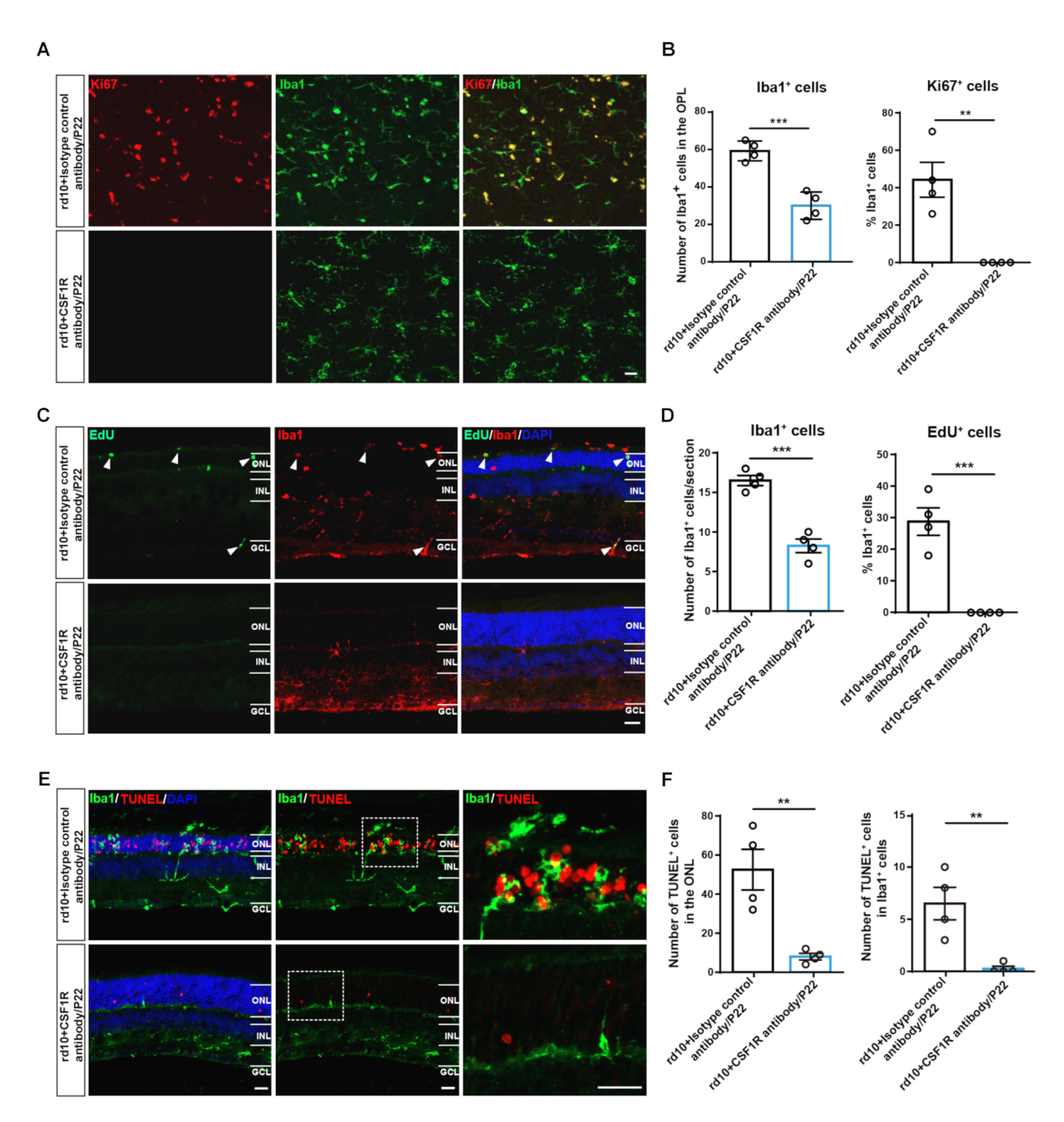


**Fig. 2** CSF1R neutralizing antibody attenuates myeloid cell proliferation in rd10 mice. (**A**) Representative confocal images showing lba1 (green) and Ki67 (red) on the retinal flat mounts of P22 rd10 mice following the intravitreal injection of a CSF1R antibody or isotype control antibody. The images were stacked images of myeloid cells located in the outer plexiform layer (OPL). Scale bar, 20 μm. (**B**) Quantification of lba1<sup>+</sup> cells (n=4 mice/group, p=0.0006). Quantification of the percentage of Ki67<sup>+</sup> cells in lba1<sup>+</sup> cells (n=4 mice/group, p=0.0032). (**C**) Representative confocal images of retinal sections from the central retina showing lba1 (red) and EdU (green) on the retinal sections of P22 rd10 mice receiving CSF1R antibody or isotype control antibody. Cell nuclei were stained with DAPI (blue). White arrowheads indicate EdU<sup>+</sup>lba1<sup>+</sup> cells. ONL: outer nuclear layer, INL: inner nuclear layer, GCL: ganglion cell layer. Scale bar, 20 μm. (**D**) Quantification of lba1<sup>+</sup> cells (n=4 mice/group, p=0.0003). Quantification of the percentage of EdU<sup>+</sup> cells in lba1<sup>+</sup> cells (n=4 mice/group, p=0.0006). (**E**) Representative confocal images of retinal sections from the central retina showing lba1 (green) and TUNEL (red) on the retinal sections of rd10 mice receiving CSF1R antibody or isotype control antibody. Scale bar, 20 μm. (**F**) Quantification of TUNEL<sup>+</sup> cells (n=4 mice/group, p=0.0055). Quantification of double-positive TUNEL<sup>+</sup> lba1<sup>+</sup> cells (n=4 mice/group, p=0.0074). Data are presented as mean±SD and analyzed using unpaired Student's t-test (B, D, F). \*\*p<0.01, \*\*\*p<0.001

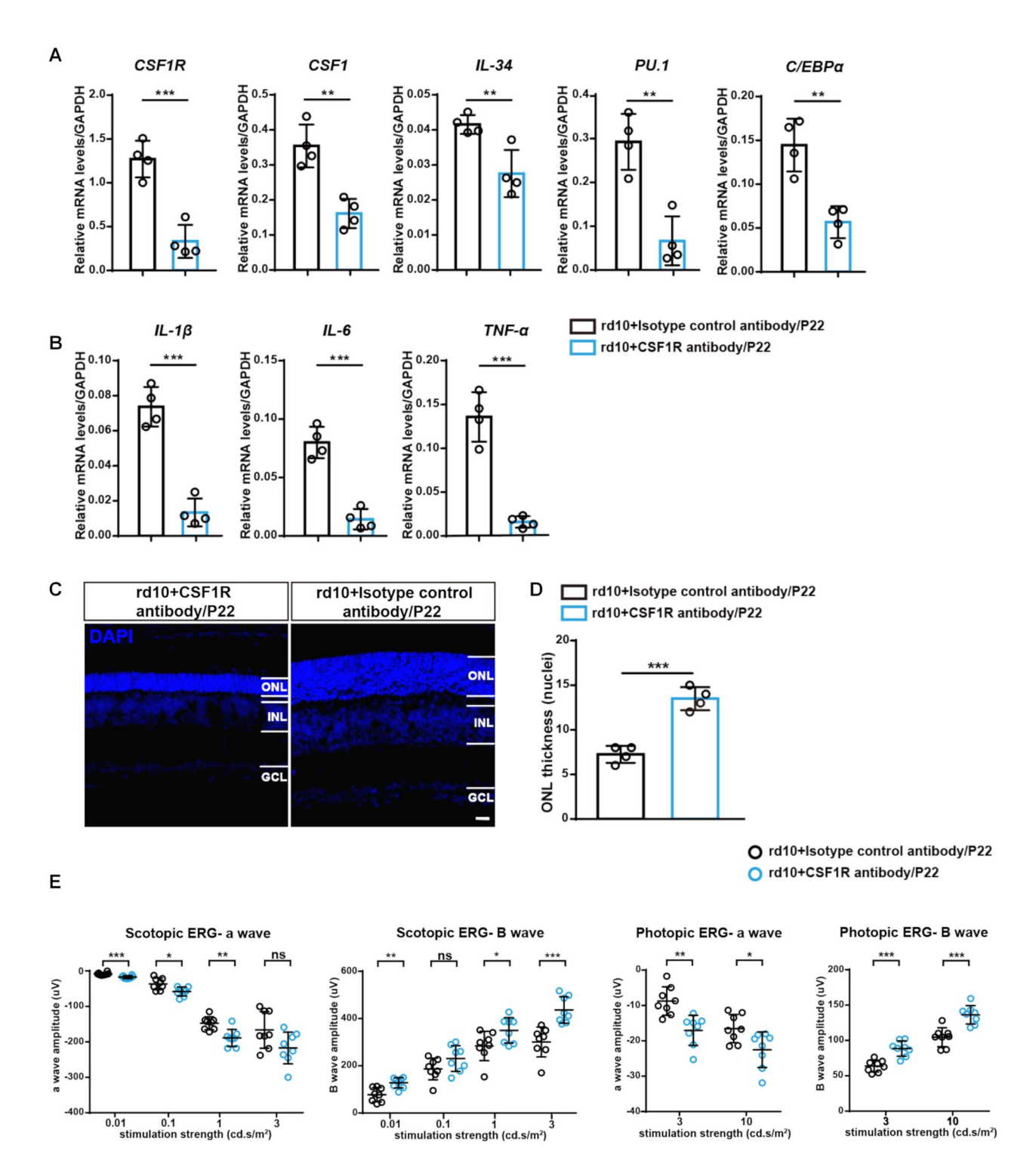


Fig. 3 (See legend on next page.)

to less Iba1<sup>+</sup> population. We observed TUNEL labelling in apoptotic photoreceptors being phagocytosed by Iba1<sup>+</sup> cells in the isotype control antibody group, whereas no TUNEL labelling in Iba1<sup>+</sup> cell nuclei were identified in anti-CSF1R group (Fig. 2E and F), indicating that

CSF1R inhibition impacts proliferation rather than survival of myeloid cells in this case. Furthermore, qPCR analysis showed that anti-CSF1R downregulated the gene expression of CSF1R signaling including CSF1R, CSF1, IL-34, PU.1, and C/EBP $\alpha$  (Fig. 3A) and pro-inflammatory

Wu et al. Journal of Neuroinflammation (2025) 22:193 Page 8 of 17

(See figure on previous page.)

**Fig. 3** CSF1R neutralizing antibody ameliorates neuroinflammation and photoreceptor degeneration in rd10 mice. (**A**) qPCR analysis of CSF1R signaling (CSF1R, p=0.0005; CSF1, p=0.002; IL-34, p=0.0083; PU.1, p=0.0018; C/EBPα, p=0.0024) and (**B**) pro-inflammatory response (IL-1β, p=0.0001; IL-6, p=0.0002; TNF-α, p=0.0002) gene expression in rd10 mice treated with CSF1R antibody or isotype control antibody (n=4 mice/group). (**C**) Representative confocal images of retinal sections from the central retina showing cell nuclei (DAPI, blue) in retinal sections of rd10 mice treated with CSF1R antibody or isotype control antibody. ONL: outer nuclear layer, INL: inner nuclear layer, GCL: ganglion cell layer. Scale bar, 20 μm. (**D**) Quantification of the number of nuclear rows in the ONL, representing photoreceptor survival between two groups (n=4 mice/group, p=0.0002). (**E**) Bar plots showing average a-wave and B-wave amplitudes in scotopic or photopic electroretinogram (ERG) responses of rd10 mice treated with CSF1R antibody or isotype control antibody (n=8 mice/group. Scotopic a-wave, 0.01 cd.s/m², p=0.0005; 0.1 cd.s/m², p=0.0017; 3 cd.s/m², p=0.0017; 3 cd.s/m², p=0.054. Scotopic B-wave, 0.01 cd.s/m², p=0.0019; 0.1 cd.s/m², p=0.0011; 1 cd.s/m², p=0.0039; 3 cd.s/m², p=0.0005. Photopic a-wave, 3 cd.s/m², p=0.0013; 10 cd.s/m², p=0.0195. Photopic B-wave, 3 cd.s/m², p=0.0001; 10 cd.s/m², p=0.0003). Data are presented as mean ± SD and analyzed using unpaired Student's t-test (**A, B, D, E**). \*p<0.05, \*\*p<0.01, \*\*\*p<0.001, ns: no significant difference

mediators including IL-1 $\beta$ , IL-6, and TNF- $\alpha$  in rd10 mice (Fig. 3B).

We further implemented systemic intervention targeting CSF1R by administering PLX5622 via daily oral gavage to rd10 mice. PLX5622 is a selective CSF1R antagonist previously shown to effectively deplete > 90% of microglia in the brain/retina following 7 days of continuous oral administration, with microglia beginning to repopulate 7 days after treatment cessation [21, 22, 29, 32]. Therefore, our treatment began from P10 to allow one-week period for PLX5622 to take effect before the onset of degeneration. Similarly, we observed less Iba1+ cells (Supplementary Fig. 1A and B) and Ki67<sup>+</sup>Iba1<sup>+</sup> cells (Supplementary Fig. 1C) in PLX5622-treated rd10 mice than those treated with corn oil. qPCR analysis revealed downregulated expression of CSF1R, PU.1, and C/EBPα, and pro-inflammatory mediators IL-1β, IL-6, and TNF-α in PLX5622-treated rd10 mice (Supplementary Fig. 1D). Together, our data suggests that both intravitreal and systemic CSF1R inhibition attenuates neurotoxic activation of myeloid cells in rd10 mice.

### CSF1R inhibition ameliorates photoreceptor degeneration and preserves visual function in rd10 mice

To evaluate the impact of CSF1R inhibition in photoreceptor survival, we assessed rod survival by measuring the thickness of ONL, which is predominantly composed of rod photoreceptors. The regions in the superior central retina that were located at 200 µm from the optic nerve head were measured. We found a thicker ONL in anti-CSF1R group compared to isotype control antibody  $(13.5 \pm 0.6 \text{ rows vs. } 7.0 \pm 0.5 \text{ rows, Fig. 3C and D}), \text{ sug-}$ gesting that CSF1R inhibition substantially preserved rod morphology. Consistently, TUNEL assay revealed fewer apoptotic photoreceptors following anti-CSF1R treatment in rd10 mice (Fig. 2E and F). Furthermore, we examined photoreceptor function by measuring electroretinograms (ERG). Scotopic ERG responses, recorded under dark-adapted conditions, primarily reflect rodpathway function responsible for vision in dim light, whereas photopic ERG responses, recorded under lightadapted conditions, predominantly assess cone-pathway function responsible for vision in bright light and color perception [33]. We found better preserved photoreceptor function following anti-CSF1R treatment in rd10 mice, with higher a-wave (scotopic 0.01, 0.1,1 cd.s/m², photopic 3, 10 cd.s/m²) and b-wave (scotopic 0.01, 1, 3 cd.s/m², photopic 3, 10 cd.s/m²) amplitudes compared to control treatment (Fig. 3E). Similarly, PLX5622 treatment in rd10 mice resulted in a significantly thicker ONL compared to corn oil treatment (14.8  $\pm$  0.5 rows vs.  $7.8 \pm 0.5$  rows, Supplementary Fig. 1E and F). We also observed improved scotopic ERG responses, but not photopic ERG responses in PLX5622-treated rd10 mice (Supplementary Fig. 1G). Collectively, our findings demonstrate that both intravitreal and systemic CSF1R inhibition effectively preserved the morphology and function of photoreceptors in rd10 retinas.

### Exogenous CSF1 or IL-34 exacerbates neuroinflammation and deteriorates visual function in rd10 mice

CSF1 and IL-34 bind to CSF1R to activate similar pathways with overlapping biological functions [34]; however, their distinct expression patterns in the retina implicate their unique roles in retinal pathologies [35]. To investigate the involvement of CSF1 and IL-34, rd10 mice received intravitreal injections of recombinant murine CSF1 or IL-34. We observed a moderate exacerbation in ONL thickness loss after recombinant IL-34 treatment, but not after recombinant CSF1R treatment, compared to control PBS treatment (Fig. 4A and B). We found no significant difference in the number of Iba1+ cells in rd10 mice treated with recombinant CSF1 or IL-34 as compared to those treated with PBS (Fig. 4C and D). However, following recombinant IL-34 treatment, we observed upregulation of CSF1R, PU.1 and C/ EBPα, along with enhanced pro-inflammatory cytokines IL-1β, IL-6, and TNF- $\alpha$  compared to PBS group (Fig. 4E). Recombinant CSF1 treatment upregulated C/EBPα and IL-1β expression with other molecules unaffected (Fig. 4E). We also found that either recombinant IL-34 or CSF1 treatment in rd10 mice led to deterioration in scotopic and photopic ERG responses (Fig. 4F). Collectively, these data suggest that the exogenous CSF1 or IL-34 exacerbates neuroinflammatory responses and impairs visual function in rd10 mice, indicating CSF1 and IL-34

Wu et al. Journal of Neuroinflammation (2025) 22:193 Page 9 of 17

combinatorially contribute to CSF1R-mediated neuro-toxicity to photoreceptors.

## Depletion of infiltrating monocyte-derived macrophages inhibits pro-inflammatory responses and protects photoreceptor function during RP

We delved deeper to illustrate the individual contributions from resident microglia and infiltrating macrophages to RP pathology through targeted depletion. CX3CR1<sup>GFP/+</sup>/rd10 mice were used for myeloid cell visualization and were administered clodronate liposomes (CL) or PBS liposomes to deplete infiltrating monocyte-derived macrophages. CL can be phagocytosed by monocytes, triggering intracellular clodronate release and subsequent cell apoptosis [36]. Because CL cannot cross the blood-retina barrier (BRB) or blood-brain barrier (BBB), it selectively depletes circulating monocytes without affecting resident microglia [37, 38]. Since the successful CL-induced depletion can usually be observed 48 h after intraperitoneal injection [39], CL was administered daily from P15 to ensure effective macrophage clearance at early stage of degeneration (Fig. 5A). We confirmed the integrity of the BRB/BBB in CL- or PBStreated CX3CR1<sup>GFP/+</sup>/rd10 mice via Evans blue dye (Supplementary Fig. 2A and B), which only penetrates the CNS if these barriers are compromised. Spleen cryosections showed sparce Iba1+F4/80+ cells in CL-treated mice compared to PBS-treated mice (Supplementary Fig. 2C), indicating effective macrophage depletion in the spleen.

Photoreceptor morphology analysis revealed moderately preserved ONL thickness in CL-treated CX3CR1<sup>GFP/+</sup>/rd10 mice compared to PBS-treated mice  $(4.8\pm0.3 \text{ rows vs. } 2.8\pm0.3 \text{ rows, Fig. 5B and C})$ . We observed less GFP+ cells (~60% reduction) in CL-treated CX3CR1<sup>GFP/+</sup>/rd10 mice (Fig. 5D and E). Less CD44 expression, a marker of infiltrating monocyte-derived macrophages facilitating their trafficking at the BRB [40], in GFP<sup>+</sup> cells verifies the depletion of infiltrating macrophages following CL treatment (Fig. 5D and E). Additionally, the expression of CSF1R signaling genes (CSF1R, CSF1, and C/EBPα) and pro-inflammatory mediators (IL-1β, IL-6, and TNF-α) was significantly reduced after CL treatment (Fig. 5F). ERG measurements also present improved retinal functionality in CL-treated mice (Fig. 5G). Together, these results suggest that infiltrating monocyte-derived macrophages partially contribute to RP pathology network potentially via modulating CSF1Rmediated neurotoxicity.

### Depletion of resident microglia preserves photoreceptor survival in RP

We next used the diphtheria toxin receptor (DTR) system to conditionally deplete resident microglia [41–44]. CX3CR1-iDTR mice were crossed with rd10 mice to

generate CX3CR1<sup>CreER/+</sup>/R26<sup>iDTR/+</sup>/rd10 mice, which were given tamoxifen (TAM) from P1-P4 to induce Cremediated recombination, followed by diphtheria toxin (DT) administration from P17-P19 to deplete cells with DTR expression (Fig. 6A). The interval between TAM and DT administration allows the selective depletion of microglia (slow turnover) while sparing macrophages (rapid turnover). The control group did not receive TAM or DT, as we have ruled out the impact of tamoxifen itself (Supplementary Fig. 3A and B). We verified that peripheral CX3CR1<sup>+</sup> populations remained intact, as indicated by comparable expression levels of Iba1 and F4/80 in spleen cryosections following microglia depletion (Supplementary Fig. 3C).

We observed less GFP<sup>+</sup> Iba1<sup>+</sup> cells (~80% reduction), retaining ramified state, in TAM/DT-treated CX3CR-1<sup>CreER/+</sup>/R26<sup>iDTR/+</sup>/rd10 mice than untreated controls (Fig. 6B and C). qPCR analysis showed mildly dampened CSF1R signaling and pro-inflammatory response, as indicated by the decreased expression of CSF1R, C/ EBPα, and TNF-α in TAM/DT-treated CX3CR1<sup>CreER/+</sup>/ R26<sup>iDTR/+</sup>/rd10 mice (Fig. 6D). Furthermore, the quantification of the ONL thickness revealed a significant preservation of photoreceptor morphology in TAM/DT-treated CX3CR1<sup>CreER/+</sup>/R26<sup>iDTR/+</sup>/rd10 mice than untreated controls  $(13.3 \pm 0.9 \text{ rows vs. } 4.0 \pm 0.6 \text{ rows, Fig. } 6\text{E} \text{ and F})$ . We also observed significantly higher a- and b-wave amplitudes following TAM/DT treatment in scotopic ERG responses (Fig. 6G), indicating preserved photoreceptors and visual function after microglia ablation. Collectively, through targeted depletion, we reported cooperative contribution of resident microglia and infiltrating macrophages in RP pathology.

### **Discussion**

CSF1R signaling is frequently implicated in microgliamediated neurodegeneration, with its role in retinal pathologies under constant debate due to conflicting evidence across various disease contexts [28, 45–47]. In the present study, we explored the role of CSF1R in the context of RP. Through pharmacological and genetic approaches, we identified CSF1R as a key regulator of neurotoxic myeloid cell activation during RP. Both intravitreal CSF1R-neutralizing antibodies and systemic PLX5622 administration achieve neuroprotection to RP. Importantly, our mechanistic study reveals a cooperative contribution of resident microglia and infiltrating macrophages to RP degeneration. These results support CSF1R as a promising combinatorial, mutation-agnostic therapeutic target for RP.

Through spatiotemporal analysis of CSF1R signaling in rd10 mice, we identified its activation specifically in disease-associated myeloid cells actively involved in degeneration process. This prompted us to investigate whether

Page 10 of 17

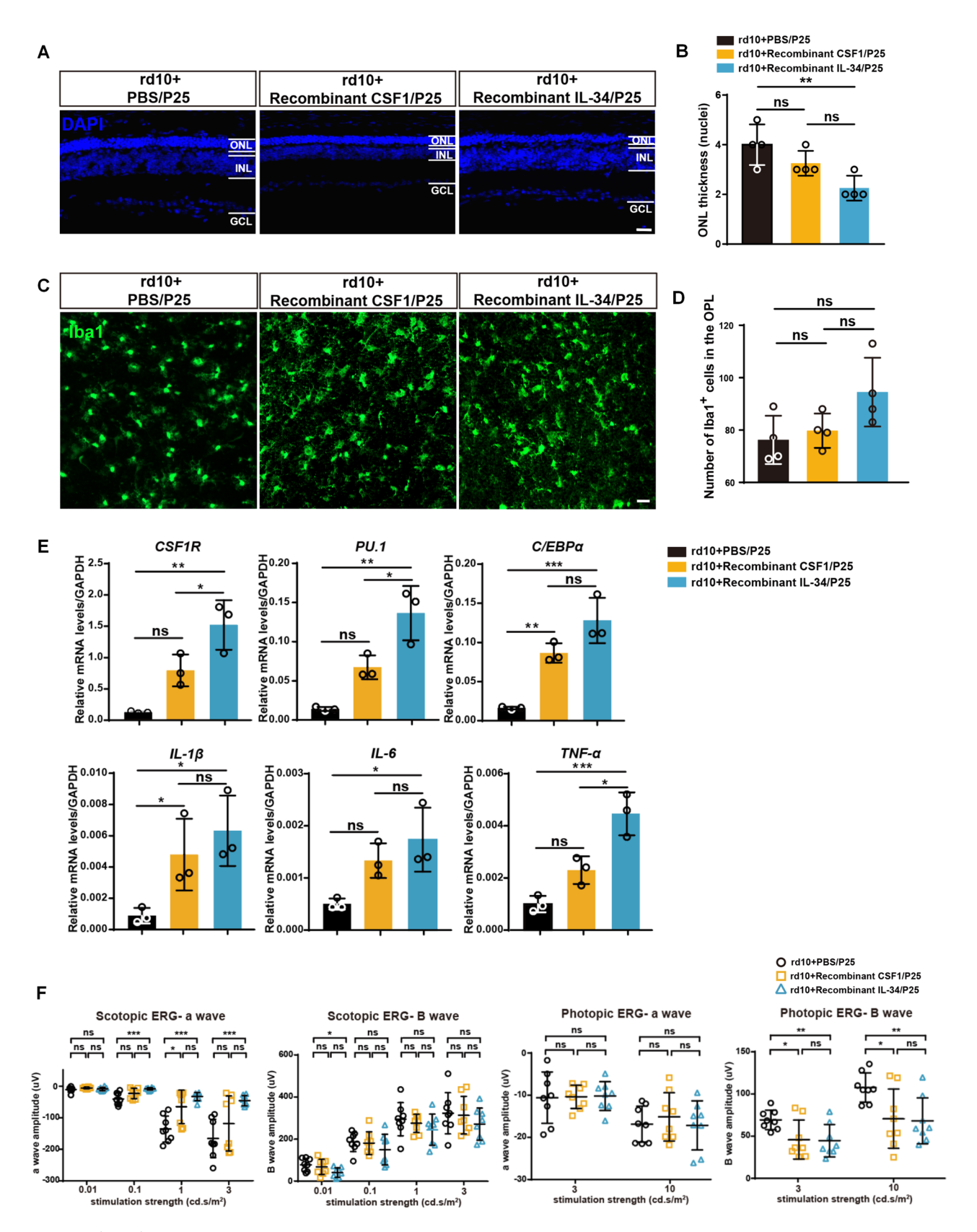


Fig. 4 (See legend on next page.)

Wu et al. Journal of Neuroinflammation (2025) 22:193 Page 11 of 17

(See figure on previous page.)

Fig. 4 Recombinant CSF1 and IL-34 deteriorates neuroinflammation and photoreceptor function in rd10 mice. (A) Representative confocal images of retinal sections from the central retina showing cell nuclei (DAPI, blue) in retinal sections of rd10 mice treated with an intravitreal injection of recombinant CSF1, IL-34, or PBS. ONL: outer nuclear layer, INL: inner nuclear layer, GCL: ganglion cell layer. Scale bar, 20 µm. (B) Quantification of the number of nuclear rows in the ONL, representing photoreceptor survival among three groups (n=4 mice/group, F(2, 9)=7.929, p=0.0103; rd10+PBS versus rd10+Re CSF1, p = 0.2569; rd10 + PBS versus rd10 + Re IL-34, p = 0.0082; rd10 + Re CSF1 versus rd10 + Re IL-34, p = 0.1124). (**C-D**) Representative confocal images and quantification of Iba1-positive myeloid cells (green) located in the outer plexiform layer (OPL) on the retinal flat mounts of rd10 mice treated with recombinant CSF1, IL-34, or PBS. Scale bar, 20  $\mu$ m. (n=4 mice/group, F(2, 9)=3.75, p=0.0654; rd10+PBS versus rd10+Re CSF1, p=0.8755; rd10+PBS versus rd10+ReIL-34, p=0.0695; rd10+Re CSF1 versus rd10+Re IL-34, p=0.1479). (E) qPCR analysis of CSF1R signaling (CSF1R, PU.1, C/EBPα) and pro-inflammatory response (IL-1 $\beta$ , IL-6, TNF- $\alpha$ ) gene expression in rd10 mice treated with recombinant CSF1, IL-34, or PBS (n=3 mice/group). CSF1R (F(2,6)=19.81, p=0.0023; rd10+PBS versus rd10+Re CSF1, p=0.0532; rd10+PBS versus rd10+Re IL-34, p=0.0018; rd10+Re CSF1 versus rd10+Re IL-34, p=0.0389). PU.1 (F(2, 6)=23.41, p=0.0015; rd10+PBS versus rd10+Re CSF1, p=0.0564; rd10+PBS versus rd10+Re IL-34, p=0.0012; rd10+Re CSF1 versus rd10+Re IL-34, p = 0.0197). C/EBP $\alpha$  (F(2, 6) = 29.07, p = 0.0008; rd10 + PBS versus rd10 + Re CSF1, p = 0.0076; rd10 + PBS versus rd10 + Re IL-34, p = 0.0007; rd10 + Re CSF1 versus rd10 + Re ||-34, p = 0.0702), ||-1 $\beta$  (F(2, 6) = 8.618, p = 0.0172; rd10 + PBS versus rd10 + Re CSF1, p = 0.0429; rd10 + PBS versus rd10 + Re ||-34, p = 0.0188; rd10 + Re CSF1 versus rd10 + Re IL-34, p = 0.772). IL-6 (F(2, 6) = 7.153, p = 0.0258; rd10 + PBS versus rd10 + Re CSF1, p = 0.102; rd10 + PBS versus rd10 + Re IL-34, p = 0.772). IL-6 (F(2, 6) = 7.153, p = 0.0258; rd10 + PBS versus rd10 + Re CSF1, p = 0.102; rd10 + PBS versus rd10 + Re IL-34, p = 0.772). IL-6 (F(2, 6) = 7.153, p = 0.0258; rd10 + PBS versus rd10 + Re CSF1, p = 0.102; rd10 + PBS versus rd10 + PBS versus rd10 +34, p = 0.0233; rd10 + Re CSF1 versus rd10 + Re IL-<math>34, p = 0.4916). TNF- $\alpha$  (F(2, 6) = 25.95, p = 0.0011; rd10 + PBS versus rd10 + Re CSF1, p = 0.0818; rd10 + PBS versus rd10 + Re CSF1, p = 0.0818; rd10 + PBS versus rd10 + Re CSF1, p = 0.0818; rd10 + Re CSF1, rd10 + Re Cversus rd10+Re IL-34, p=0.0009, rd10+Re CSF1 versus rd10+Re IL-34, p=0.0102). (F) Bar plots showing average a-wave and B-wave amplitudes in scotopic or photopic electroretinogram (ERG) responses of rd10 mice treated with recombinant CSF1, IL-34, or PBS (n=8 mice/group) (For the statistical values, please refer to supplementary file 3). Data are presented as mean ± SD and analyzed using One way ANOVA with Tukey's post hoc test (B, D, E, F). \*p < 0.05, \*\*p < 0.01, \*\*\*p < 0.001, ns: no significant difference

CSF1R inhibition could have a protective effect. Combinatorial evidence from intravitreal anti-CSF1R treatment and systemic PLX5622 administration showed that CSF1R inhibition reduced proliferation and activation of myeloid cells, inhibited pro-inflammatory responses, and effectively preserved photoreceptor survival and visual function. Contrary to the prevalent perspective that CSF1R inhibition primarily depletes microglia to achieve its effects [48, 49], our study suggests that CSF1R inhibition notably restrained myeloid cell proliferation to bring its impact in RP. This hypothesis is supported by: (1) CSF1R activation coincides with dramatic expansion of myeloid cells; (2) Post CSF1R inhibition in rd10 mice, the number of myeloid cells dropped to a level comparable to untreated control C57BL/6J mice; (3) Downregulation of PU.1 and  $C/EBP\alpha$  - transcription factors pivotal for the pro-mitogenic program [24]; (4) a decrease in EdU<sup>+</sup> cells and Ki67<sup>+</sup> cells; (5) Undetectable TUNEL<sup>+</sup>Iba<sup>+</sup> cells upon CSF1R inhibition in rd10 mice. The predominant role of CSF1R in myeloid cell proliferation rather than depletion could be attributed to varying pathological contexts [24, 25, 50], the robust self-renewal capability of microglia [51], and the specific strategies employed for CSF1R inhibition (intervention approach, dose-ranging, and timing)

IL-34 and CSF1 activate CSF1R in a similar fashion, but showing distinct expression pattern depending on niche and health/disease conditions [52–55]. In homeostatic retinas, IL-34 is selectively expressed by retinal ganglion cells to support the survival of microglia located in the inner plexiform layer (IPL), thereby contributing to visual function [35]. However, the functionality of IL-34 and CSF1 in retinal pathologies remains unidentified. Here, we introduced exogenous IL-34 and CSF1 into rd10 eyes and observed escalation of pro-inflammatory responses and impaired photoreceptor function without further accumulation of myeloid cells. It is possible that myeloid

cells already reached their maximum proliferation capacity during the peak of degeneration, which could be restricted by factors including nutritional support, cell cycle constraints, and other transcription regulatory elements [56-59]. Based on our data, we suspect an overlapping function of IL-34 and CSF1 in pro-inflammatory cytokine production. But the unique expression dynamic of IL-34, upregulated in the early and downregulated in the peak stage of RP, also implicates other non-overlapping roles during RP progression. To further investigate the functional divergence between IL-34 and CSF1 in the near future, we propose using genetic models such as IL-34<sup>LacZ/LacZ</sup> mice [60] or CSF1<sup>fl/fl</sup> mice [61], crossed with inducible CreER lines targeting specific myeloid cell populations, and subsequently bred onto a RP genetic background. This approach would enable precise dissection of ligand-dependent effects on retinal degeneration and neuroinflammation.

Our work unravels a concurrent contribution of resident microglia and infiltrating monocyte-derived macrophages to RP pathology, but interesting differences exist between the two scenarios. In the case of resident microglia depletion, we found more than 80% preservation in ONL thickness and substantial preservation of scotopic ERG responses. Such a strong protective efficacy is likely attributed to resident microglia being the primary responder to local stimuli and crucial recruiter of circulating macrophages. However, despite an obvious preservation in cone morphology (data not shown), we did not identify difference in photopic ERG responses following microglia depletion. A similar phenomenon was also observed after PLX5622 administration. One possible explanation is that cones may be more dependent on supportive microglia-derived factors or more sensitive to microglial loss than rods. Systemic PLX5622 may suppress microglial proliferation and inflammatory activation but also compromise beneficial or homeostatic Wu et al. Journal of Neuroinflammation (2025) 22:193 Page 12 of 17

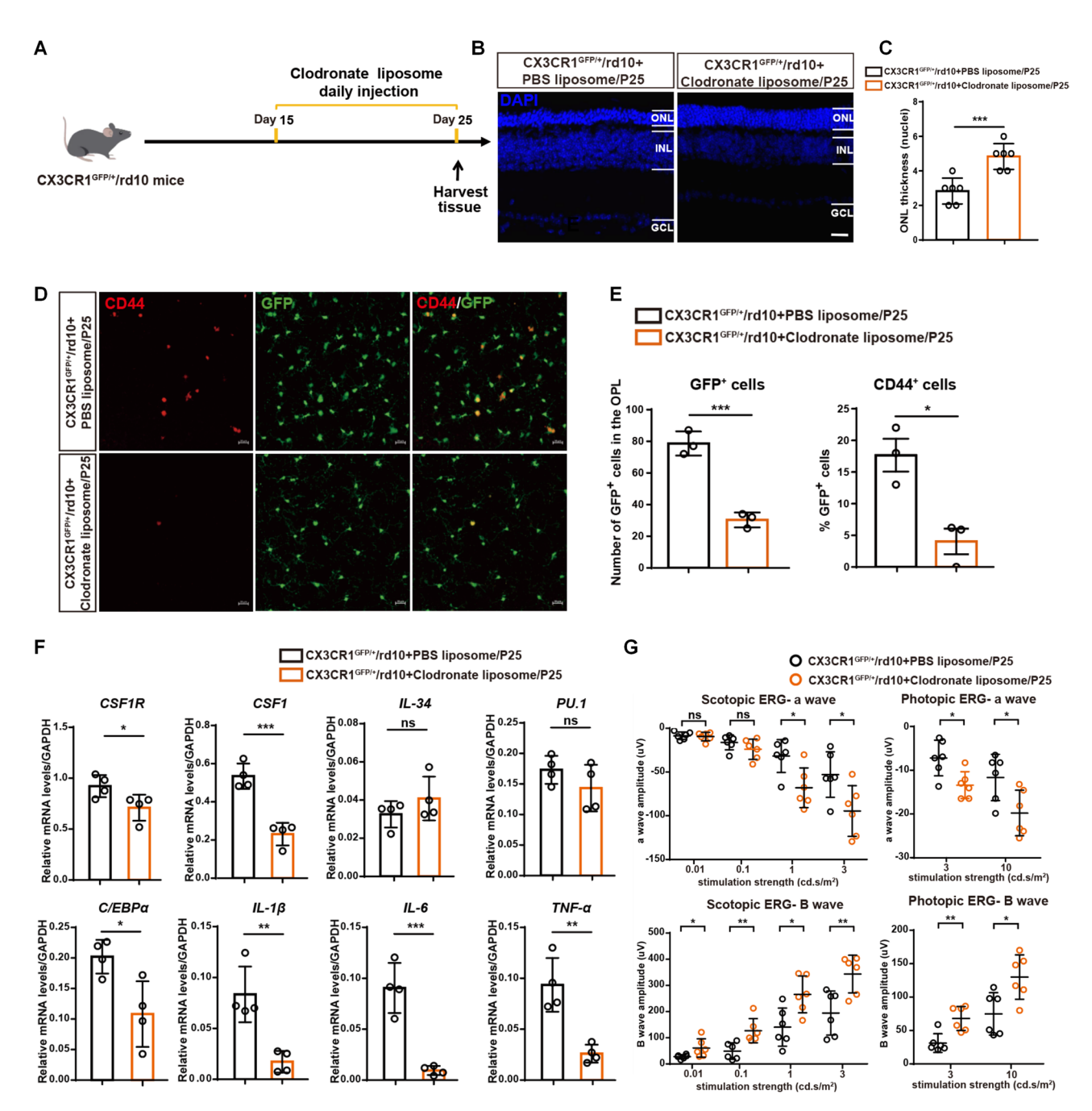


Fig. 5 Infiltrating monocyte depletion via clodronate liposome inhibits pro-inflammatory response and protects photoreceptor functions during RP. (A) Scheme of clodronate liposome (CL) administration and time points for observation. (B) Representative confocal images of retinal sections from the central retina showing cell nuclei (DAPI, blue) in retinal sections of CX3CR1 GFP/+/rd10 mice treated with daily intraperitoneal injection of clodronate liposome or PBS liposome. ONL: outer nuclear layer, INL: inner nuclear layer, GCL: ganglion cell layer. Scale bar, 20 μm. (C) Quantification of the number of nuclear rows in the ONL, representing photoreceptor survival between two groups (n=6 mice/group, p=0.001). (D) Representative confocal images showing GFP (green) and CD44 (red) on the retinal flat mounts of CX3CR1 GFP/+/rd10 mice treated with clodronate liposome or PBS liposome. The images were stacked images of myeloid cells located in the outer plexiform layer (OPL). Scale bar, 20 μm. (E) Quantification of GFP+ cells (n=3 mice/group, p=0.0007). Quantification of the percentage of CD44+ cells in GFP+ cells (n=3 mice/group, p=0.0144). (F) qPCR analysis of CSF1R signaling (CSF1R, p=0.0453; CSF1, p=0.0005; lL-34, p=0.2607; PU.1, p=0.2323; C/EBPα, p=0.0299) and pro-inflammatory response (lL-1β, p=0.0041; lL-6, p=0.0006; TNF-α, p=0.0028) gene expression in CX3CR1 GFP/+/rd10 mice treated with clodronate liposome or PBS liposome (n=4 mice/group). (G) Bar plots showing average a-wave and B-wave amplitudes in scotopic or photopic electroretinogram (ERG) responses of CX3CR1 GFP/+/rd10 mice treated with clodronate liposome or PBS liposome (n=6 mice/group, scotopic a-wave, 0.01 cd.s/m², p=0.0327, p=0.0327,

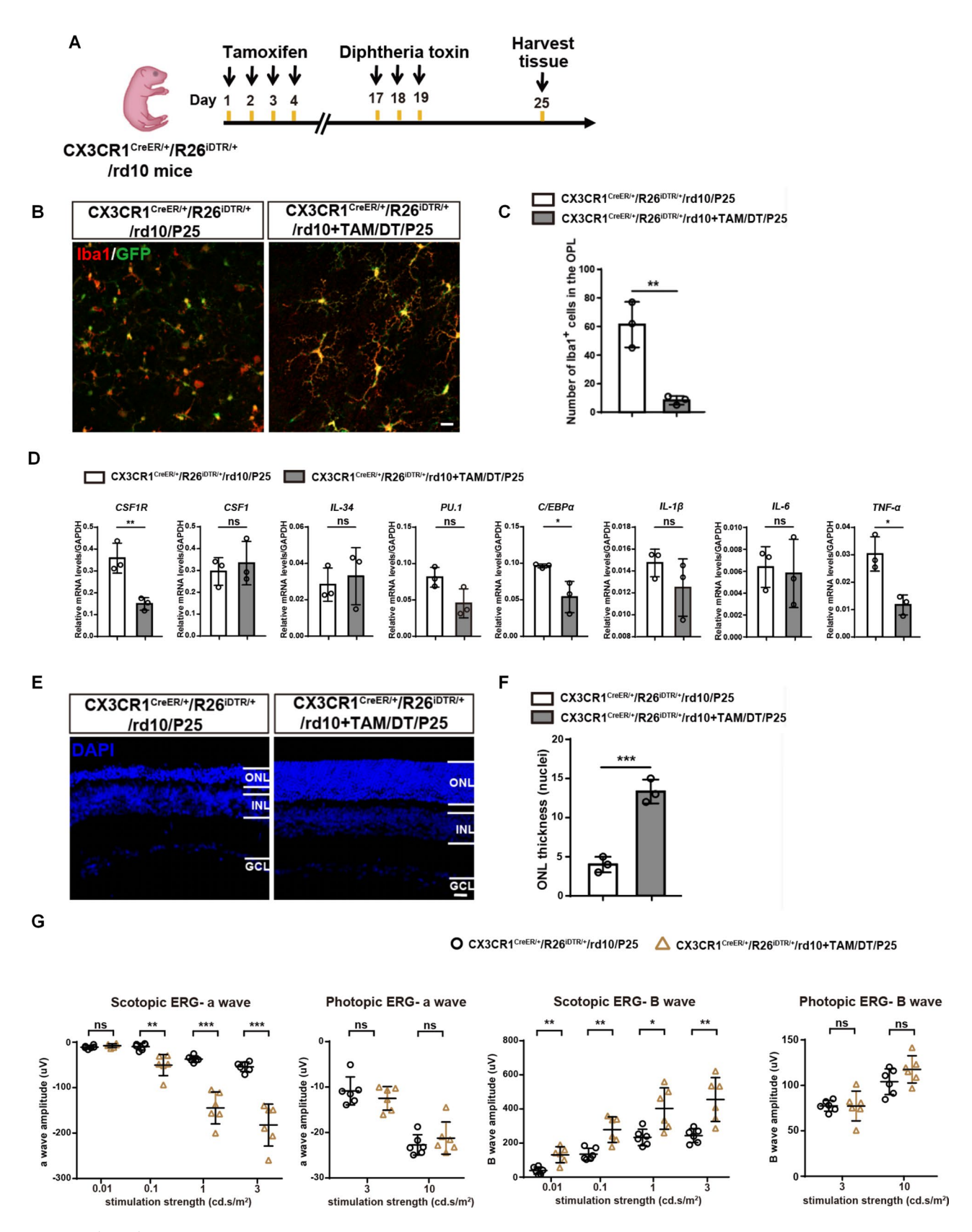


Fig. 6 (See legend on next page.)

Wu et al. Journal of Neuroinflammation (2025) 22:193 Page 14 of 17

(See figure on previous page.)

**Fig. 6** Resident microglia deletion protects photoreceptors and retinal functions during RP. (**A**) Scheme of tamoxifen (TAM) and diphtheria toxin (DT) administration in CX3CR1<sup>CreER/+</sup>/R26<sup>iDTR/+</sup>/rd10 mice to deplete resident microglia and time points for observation. (**B**) Representative confocal images showing GFP (green) and Iba1 (red) on the retinal flat mounts of TAM/DT-treated or untreated CX3CR1<sup>CreER/+</sup>/R26<sup>iDTR/+</sup>/rd10 mice. The images were stacked images located in the outer plexiform layer (OPL). Scale bar, 20 μm. (**C**) Quantification of Iba1<sup>+</sup> cells in the OPL (n=3 mice/group, p=0.0049). (**D**) qPCR analysis of CSF1R signaling (CSF1R, p=0.0082; CSF1, p=0.06057; IL-34, p=0.06802; PU.1, p=0.0608; C/EBPα, p=0.0267) and pro-inflammatory response (IL-1β, p=0.2504; IL-6, p=0.7938; TNF-a, p=0.0113) gene expression in TAM/DT-treated or untreated CX3CR1<sup>CreER/+</sup>/R26<sup>iDTR/+</sup>/rd10 mice (n=3 mice/group). (**E**) Representative confocal images of retinal sections from the central retina showing cell nuclei (DAPI, blue) in retinal sections of TAM/DT-treated or untreated CX3CR1<sup>CreER/+</sup>/R26<sup>iDTR/+</sup>/rd10 mice. ONL: outer nuclear layer, INL: inner nuclear layer, GCL: ganglion cell layer. Scale bar, 20 μm. (**F**) Quantification of the number of nuclear rows in the ONL, representing photoreceptor survival (n=3 mice/group, p=0.0009). (**G**) Bar plots showing average a- and B-wave amplitudes in scotopic or photopic electroretinogram (ERG) responses of TAM/DT-treated or untreated CX3CR1<sup>CreER/+</sup>/R26<sup>iDTR/+</sup>/rd10 mice (n=6 mice/group, scotopic a-wave, 0.01 cd.s/m², p=0.1844; 0.1 cd.s/m², p=0.0023; 1 cd.s/m², p<0.0001; 3 cd.s/m², p<0.0001; 3 cd.s/m², p=0.3452; 10 cd.s/m², p=0.04025. Photopic B-wave, 3 cd.s/m², p=0.9885; 10 cd.s/m², p=0.14). Data are presented as mean ±SD and analyzed using unpaired Student's *t*-test (**C, D, F, G**). \*p<0.005, \*\*p<0.001, ns: no significant difference

microglial functions, particularly those important for cone maintenance. Indeed, Wang et al. found that although microglia are not acutely necessary for retinal architecture or neuron survival, their prolonged absence can lead to photoreceptor synapse degeneration and subsequent functional decline to light response [62]. Funatsu et al. also reported that PLX5622 administration from P21 to P31 in rd10 mice resulted in almost complete depletion of microglia and decrease of cone density [20]. Therefore, a delicate balance exists between the beneficial effects from less microglia-derived neurotoxicity and the detrimental impact from compromised synaptic function due to microglia depletion, a topic that warrants further investigation.

In the case of infiltrating monocyte-derived macrophage depletion, we observed a relative mild impact in rod protection. Instead, we observed a significant suppression in pro-inflammatory cytokine expression. This aligns with multiple studies showing that knockout of CCL2/CCR2, crucial axis for monocyte recruitment, resulted in mild photoreceptor degeneration and significant decreased expression of pro-inflammatory mediators like NLRP3, IL-1 $\beta$ , MCP1 [63, 64]. Zhao et al. also reported that infiltrating macrophages contribute less to the phagocytic clearance of photoreceptors than resident microglia [9]. Therefore, we propose that monocytederived macrophages preferentially contribute to RP pathology via secretion of neurotoxic mediators.

We acknowledge that while CSF1R plays a significant role in regulating myeloid cell behavior in RP, it is part of a broader regulatory landscape. Microglial activation and neuroinflammation are regulated by a complex network of upstream and parallel pathways, including TREM2, CX3CR1, TAK1, COX-1, TLR signaling [8, 10, 19, 65, 66], which may interact with or operate independently of CSF1R. Moreover, the current study relies on pharmacological intervention to modulate CSF1R and employs cell ablation strategies to infer synergy between resident microglia and infiltrating macrophages. While these approaches provide valuable insights, several key mechanistic questions remain to be resolved. Specifically: (1)

the dominant contribution of either resident microglia or infiltrating macrophages in driving neuroinflammation has not been clearly defined; (2) the nature of crosstalk between these two populations—whether their effects are additive, synergistic, parallel, or mediated through direct or indirect communication—remains to be elucidated; and (3) the differential impact of CSF1R signaling on microglia versus macrophages in the degenerative retina is not yet fully understood. To address these gaps, future studies might incorporate strategies with greater cellular and molecular resolution. This includes the use of more specific markers (e.g. Tmem119, P2ry12 for microglia; CD45<sup>high</sup>, CD11b<sup>+</sup>Ly6c<sup>+</sup> for infiltrating macrophages), high resolution approaches like single-cell RNA sequencing [13], and fate mapping techniques using transgenic mouse models like Tmem119<sup>CreERT2</sup> (targeting resident microglia) [67] and CCR2<sup>CreER</sup> (targeting monocytes) [68]. These tools will be critical for deepening mechanistic understanding and guiding the rational design of targeted therapies for retinal degeneration.

Although we provide evidence that CSF1R inhibition offers a valid path to mitigate RP pathology, several translational challenges must be addressed. Safety and target specificity remain critical concerns, as CSF1R is broadly expressed in peripheral macrophages, and systemic or off-target inhibition may cause unintended immune suppression and tissue dysfunction [69, 70]. The long-term effects of modulating myeloid CSF1R activity also remain unclear. Additionally, optimizing therapeutic timing, dosage, and delivery is essential, especially given that our findings only implicate preventive efficacy at early stages of degeneration and detailed pharmacokinetic data are lacking. Demonstrating mutation-agnostic efficacy and identifying responsive patient subgroups will require validation in animal models [71] and patient-derived iPSC retinal organoids with diverse genetic backgrounds [72, 73]. Notably, the favorable outcomes of minocycline, an antibiotic known to suppress microglial activation and proliferation, in a recent RP clinical trial [12] reinforce our hypothesis that targeting microglia/myeloid pathways represents a viable, mutation-independent therapeutic strategy [8]. We remain confident that, upon overcoming these translational hurdles, dual-targeting CSF1R signaling holds strong potential for RP treatment.

### **Supplementary Information**

The online version contains supplementary material available at https://doi.or q/10.1186/s12974-025-03525-0.

Supplementary Material 1

Supplementary Material 2

Supplementary Material 3

### Acknowledgements

We thank the University Research Facility in Life Sciences (ULS) and University Research Facility in Behavioral and Systems Neuroscience (UBSN) of the Hong Kong Polytechnic University for providing access to advanced instruments needed for this study.

#### **Author contributions**

This study was designed by JW, JZ, and BL. The experiments were performed by JW. The experimental data were analyzed by JW and JZ. The manuscript was drafted by JZ, and revised by JW and BL. All authors read and approved the final manuscript.

#### **Funding**

BL was kindly supported by General Research Fund (GRF) from the Hong Kong Research Grants Council, the Health and Medical Research Fund (HMRF) of Hong Kong Food and Health Bureau, and Project of Strategic Importance of The Hong Kong Polytechnic University. This study was supported by the Centre for Eye and Vision Research Ltd (CEVR) and the InnoHK initiative of the Innovation and Technology Commission of the Hong Kong Special Administrative Region Government.

### Data availability

Data is provided within the manuscript or supplementary information files.

### **Declarations**

### Ethics approval and consent to participate

All experimental procedures were approved by the Animal Subjects Ethics Sub-committee (ASESC) of Hong Kong Polytechnic University and conducted in accordance with the Association for Research in Vision and Ophthalmology (ARVO) statement for the use of animals.

### Consent for publication

Not applicable.

### Competing interests

The authors declare no competing interests.

Received: 18 May 2025 / Accepted: 20 July 2025 Published online: 26 July 2025

### References

- Dias MF, Joo K, Kemp JA, Fialho SL, da Silva Cunha A Jr., Woo SJ, et al. Molecular genetics and emerging therapies for retinitis pigmentosa: basic research and clinical perspectives. Prog Retin Eye Res. 2018;63:107–31. https://doi.org/10.1016/j.preteyeres.2017.10.004.
- Hartong DT, Berson EL, Dryja TP, Retinitis pigmentosa. Lancet. 2006;368(9549):1795–809. https://doi.org/10.1016/S0140-6736(06)69740-7.
- Ferrari S, Di Iorio E, Barbaro V, Ponzin D, Sorrentino FS, Parmeggiani F. Retinitis pigmentosa: genes and disease mechanisms. Curr Genomics. 2011;12(4):238– 49. https://doi.org/10.2174/138920211795860107.
- Sahni JN, Angi M, Irigoyen C, Semeraro F, Romano MR, Parmeggiani F. Therapeutic challenges to retinitis pigmentosa: from neuroprotection to gene

- therapy. Curr Genomics. 2011;12(4):276–84. https://doi.org/10.2174/1389202 11795860062.
- Daiger SP, Bowne SJ, Sullivan LS. Perspective on genes and mutations causing retinitis pigmentosa. Arch Ophthalmol. 2007;125(2):151–8. https://doi.org/10. 1001/archopht.125.2.151.
- Anasagasti A, Irigoyen C, Barandika O, Lopez de Munain A, Ruiz-Ederra J. Current mutation discovery approaches in retinitis pigmentosa. Vis Res. 2012;75:117–29. https://doi.org/10.1016/j.visres.2012.09.012.
- Schneider N, Sundaresan Y, Gopalakrishnan P, Beryozkin A, Hanany M, Levanon EY, et al. Inherited retinal diseases: linking genes, disease-causing variants, and relevant therapeutic modalities. Prog Retin Eye Res. 2022;89:101029. https://doi.org/10.1016/j.preteyeres.2021.101029.
- Peng B, Xiao J, Wang K, So KF, Tipoe GL, Lin B. Suppression of microglial activation is neuroprotective in a mouse model of human retinitis pigmentosa. J Neurosci. 2014;34(24):8139–50. https://doi.org/10.1523/JNEUROSCI.5200-13.2 014.
- Zhao L, Zabel MK, Wang X, Ma W, Shah P, Fariss RN, et al. Microglial phagocytosis of living photoreceptors contributes to inherited retinal degeneration. EMBO Mol Med. 2015;7(9):1179–97. https://doi.org/10.15252/emmm.201505298
- Yang W, Xiong G, Lin B. Cyclooxygenase-1 mediates neuroinflammation and neurotoxicity in a mouse model of retinitis pigmentosa. J Neuroinflammation. 2020;17(1):306. https://doi.org/10.1186/s12974-020-01993-0.
- Yang H, Zhang H, Li X. Navigating the future of retinitis pigmentosa treatments: A comprehensive analysis of therapeutic approaches in rd10 mice. Neurobiol Dis. 2024;193:106436. https://doi.org/10.1016/j.nbd.2024.106436.
- Chen Y, Pan Y, Xie Y, Shi Y, Lu Y, Xia Y, et al. Efficacy and safety of Minocycline in retinitis pigmentosa: a prospective, open-label, single-arm trial. Signal Transduct Target Ther. 2024;9(1):339. https://doi.org/10.1038/s41392-024-020 37-2.
- Yu C, Roubeix C, Sennlaub F, Saban DR. Microglia versus monocytes: distinct roles in degenerative diseases of the retina. Trends Neurosci. 2020;43(6):433– 49. https://doi.org/10.1016/j.tins.2020.03.012.
- Gupta N, Brown KE, Milam AH. Activated microglia in human retinitis pigmentosa, late-onset retinal degeneration, and age-related macular degeneration. Exp Eye Res. 2003;76(4):463–71. https://doi.org/10.1016/s0014-4835(02)0033 2-9.
- Zabel MK, Zhao L, Zhang Y, Gonzalez SR, Ma W, Wang X, et al. Microglial phagocytosis and activation underlying photoreceptor degeneration is regulated by CX3CL1-CX3CR1 signaling in a mouse model of retinitis pigmentosa. Glia. 2016;64(9):1479–91. https://doi.org/10.1002/glia.23016.
- Yoshida N, Ikeda Y, Notomi S, Ishikawa K, Murakami Y, Hisatomi T, et al. Clinical evidence of sustained chronic inflammatory reaction in retinitis pigmentosa. Ophthalmology. 2013;120(1):100–5. https://doi.org/10.1016/j.ophtha.2012.07. 006.
- Zeng HY, Zhu XA, Zhang C, Yang LP, Wu LM, Tso MO. Identification of sequential events and factors associated with microglial activation, migration, and cytotoxicity in retinal degeneration in Rd mice. Invest Ophthalmol Vis Sci. 2005;46(8):2992–9. https://doi.org/10.1167/iovs.05-0118.
- Zhao L, Hou C, Yan N. Neuroinflammation in retinitis pigmentosa: therapies targeting the innate immune system. Front Immunol. 2022;13:1059947. https://doi.org/10.3389/fimmu.2022.1059947.
- Zhang J, Yang W, Wu J, Lin B. Understanding TAK1 deficiency in microglia: dual mechanisms for photoreceptor protection in a mouse model of retinitis pigmentosa. Proc Natl Acad Sci U S A. 2025;122(18):e2423134122. https://doi. org/10.1073/pnas.2423134122.
- Funatsu J, Murakami Y, Shimokawa S, Nakatake S, Fujiwara K, Okita A, et al. Circulating inflammatory monocytes oppose microglia and contribute to cone cell death in retinitis pigmentosa. PNAS Nexus. 2022;1(1). https://doi.org/10.1093/pnasnexus/pgac003.
- 21. Elmore MR, Najafi AR, Koike MA, Dagher NN, Spangenberg EE, Rice RA, et al. Colony-stimulating factor 1 receptor signaling is necessary for microglia viability, unmasking a microglia progenitor cell in the adult brain. Neuron. 2014;82(2):380–97. https://doi.org/10.1016/j.neuron.2014.02.040.
- Huang Y, Xu Z, Xiong S, Qin G, Sun F, Yang J, et al. Dual extra-retinal origins of microglia in the model of retinal microglia repopulation. Cell Discov. 2018;4:9. https://doi.org/10.1038/s41421-018-0011-8.
- Han J, Chitu V, Stanley ER, Wszolek ZK, Karrenbauer VD, Harris RA. Inhibition of colony stimulating factor-1 receptor (CSF-1R) as a potential therapeutic strategy for neurodegenerative diseases: opportunities and challenges. Cell Mol Life Sci. 2022;79(4):219. https://doi.org/10.1007/s00018-022-04225-1.

- Olmos-Alonso A, Schetters ST, Sri S, Askew K, Mancuso R, Vargas-Caballero M, et al. Pharmacological targeting of CSF1R inhibits microglial proliferation and prevents the progression of Alzheimer's-like pathology. Brain. 2016;139(Pt 3):891–907. https://doi.org/10.1093/brain/awv379.
- Gomez-Nicola D, Fransen NL, Suzzi S, Perry VH. Regulation of microglial proliferation during chronic neurodegeneration. J Neurosci. 2013;33(6):2481–93. https://doi.org/10.1523/JNEUROSCI.4440-12.2013.
- Hu B, Duan S, Wang Z, Li X, Zhou Y, Zhang X, et al. Insights into the role of CSF1R in the central nervous system and neurological disorders. Front Aging Neurosci. 2021;13:789834. https://doi.org/10.3389/fnagi.2021.789834.
- Gerber YN, Saint-Martin GP, Bringuier CM, Bartolami S, Goze-Bac C, Noristani HN, et al. CSF1R Inhibition reduces microglia proliferation, promotes tissue preservation and improves motor recovery after spinal cord injury. Front Cell Neurosci. 2018;12:368. https://doi.org/10.3389/fncel.2018.00368.
- Tang Y, Xiao Z, Pan L, Zhuang D, Cho KS, Robert K, et al. Therapeutic targeting of retinal immune microenvironment with CSF-1 receptor antibody promotes visual function recovery after ischemic optic neuropathy. Front Immunol. 2020;11:585918. https://doi.org/10.3389/fimmu.2020.585918.
- Okunuki Y, Mukai R, Nakao T, Tabor SJ, Butovsky O, Dana R, et al. Retinal microglia initiate neuroinflammation in ocular autoimmunity. Proc Natl Acad Sci U S A. 2019;116(20):9989–98. https://doi.org/10.1073/pnas.1820387116.
- Rahman-Enyart A, Yaggie RE, Bollinger JL, Arvanitis C, Winter DR, Schaeffer AJ, et al. Acyloxyacyl hydrolase regulates microglia-mediated pelvic pain. PLoS ONE. 2022;17(8):e0269140. https://doi.org/10.1371/journal.pone.0269140.
- Chang B, Hawes NL, Hurd RE, Davisson MT, Nusinowitz S, Heckenlively JR. Retinal degeneration mutants in the mouse. Vis Res. 2002;42(4):517–25. https://doi.org/10.1016/s0042-6989(01)00146-8.
- 32. Wang M, Caryotakis SE, Smith GG, Nguyen AV, Pleasure DE, Soulika AM. CSF1R antagonism results in increased supraspinal infiltration in EAE. J Neuroinflammation. 2024;21(1):103. https://doi.org/10.1186/s12974-024-03063-1.
- Robson AG, Frishman LJ, Grigg J, Hamilton R, Jeffrey BG, Kondo M, et al. ISCEV standard for full-field clinical electroretinography (2022 update). Doc Ophthalmol. 2022;144(3):165–77. https://doi.org/10.1007/s10633-022-0987 2-0.
- Stanley ER, Chitu V. CSF-1 receptor signaling in myeloid cells. Cold Spring Harb Perspect Biol. 2014;6(6). https://doi.org/10.1101/cshperspect.a021857.
- O'Koren EG, Yu C, Klingeborn M, Wong AYW, Prigge CL, Mathew R, et al. Microglial function is distinct in different anatomical locations during retinal homeostasis and degeneration. Immunity. 2019;50(3):723–37. https://doi.org/10.1016/j.immuni.2019.02.007. e7.
- van Rooijen N, Sanders A, van den Berg TK. Apoptosis of macrophages induced by liposome-mediated intracellular delivery of clodronate and Propamidine. J Immunol Methods. 1996;193(1):93–9. https://doi.org/10.1016/ 0022-1759(96)00056-7.
- Huitinga I, Damoiseaux JG, van Rooijen N, Dopp EA, Dijkstra CD. Liposome mediated affection of monocytes. Immunobiology. 1992;185(1):11–9. https://doi.org/10.1016/S0171-2985(11)80313-X.
- Sakurai E, Anand A, Ambati BK, van Rooijen N, Ambati J. Macrophage depletion inhibits experimental choroidal neovascularization. Invest Ophthalmol Vis Sci. 2003;44(8):3578–85. https://doi.org/10.1167/iovs.03-0097.
- Nguyen T, Du J, Li YC. A protocol for macrophage depletion and reconstitution in a mouse model of sepsis. STAR Protoc. 2021;2(4):101004. https://doi.org/10.1016/j.xpro.2021.101004.
- Xu H, Manivannan A, Liversidge J, Sharp PF, Forrester JV, Crane IJ. Involvement of CD44 in leukocyte trafficking at the blood-retinal barrier. J Leukoc Biol. 2002;72(6):1133–41.
- 41. Goto Y, Hogg JC, Suwa T, Quinlan KB, van Eeden SF. A novel method to quantify the turnover and release of monocytes from the bone marrow using the thymidine analog 5'-bromo-2'-deoxyuridine. Am J Physiol Cell Physiol. 2003;285(2):C253–9. https://doi.org/10.1152/ajpcell.00035.2003.
- Parkhurst CN, Yang G, Ninan I, Savas JN, Yates JR 3rd, Lafaille JJ, et al. Microglia promote learning-dependent synapse formation through brain-derived neurotrophic factor. Cell. 2013;155(7):1596–609. https://doi.org/10.1016/j.cell. 2013.11.030.
- 43. van Furth R. Origin and turnover of monocytes and macrophages. Curr Top Pathol. 1989;79:125–50.
- Yona S, Kim KW, Wolf Y, Mildner A, Varol D, Breker M, et al. Fate mapping reveals origins and dynamics of monocytes and tissue macrophages under homeostasis. Immunity. 2013;38(1):79–91. https://doi.org/10.1016/j.immuni.2 012.12.001.
- 45. Kokona D, Ebneter A, Escher P, Zinkernagel MS. Colony-stimulating factor 1 receptor Inhibition prevents disruption of the blood-retina barrier during

- chronic inflammation. J Neuroinflammation. 2018;15(1):340. https://doi.org/10.1186/s12974-018-1373-4.
- Okunuki Y, Mukai R, Pearsall EA, Klokman G, Husain D, Park DH, et al. Microglia inhibit photoreceptor cell death and regulate immune cell infiltration in response to retinal detachment. Proc Natl Acad Sci U S A. 2018;115(27):E6264–73. https://doi.org/10.1073/pnas.1719601115.
- Todd L, Palazzo I, Suarez L, Liu X, Volkov L, Hoang TV, et al. Reactive microglia and IL1beta/IL-1R1-signaling mediate neuroprotection in excitotoxin-damaged mouse retina. J Neuroinflammation. 2019;16(1):118. https://doi.org/10.1 186/s12974-019-1505-5.
- Spangenberg E, Severson PL, Hohsfield LA, Crapser J, Zhang J, Burton EA, et al. Sustained microglial depletion with CSF1R inhibitor impairs parenchymal plaque development in an alzheimer's disease model. Nat Commun. 2019;10(1):3758. https://doi.org/10.1038/s41467-019-11674-z.
- Sosna J, Philipp S, Albay R 3rd, Reyes-Ruiz JM, Baglietto-Vargas D, LaFerla FM, et al. Early long-term administration of the CSF1R inhibitor PLX3397 ablates microglia and reduces accumulation of intraneuronal amyloid, neuritic plaque deposition and pre-fibrillar oligomers in 5XFAD mouse model of alzheimer's disease. Mol Neurodegener. 2018;13(1):11. https://doi.org/10.118 6/s13024-018-0244-x.
- Chitu V, Gokhan S, Nandi S, Mehler MF, Stanley ER. Emerging roles for CSF-1 receptor and its ligands in the nervous system. Trends Neurosci. 2016;39(6):378–93. https://doi.org/10.1016/j.tins.2016.03.005.
- Bruttger J, Karram K, Wortge S, Regen T, Marini F, Hoppmann N, et al. Genetic cell ablation reveals clusters of local Self-Renewing microglia in the mammalian central nervous system. Immunity. 2015;43(1):92–106. https://doi.org/ 10.1016/Limmuni.2015.06.012.
- Easley-Neal C, Foreman O, Sharma N, Zarrin AA, Weimer RM. CSF1R ligands IL-34 and CSF1 are differentially required for microglia development and maintenance in white and Gray matter brain regions. Front Immunol. 2019;10:2199. https://doi.org/10.3389/fimmu.2019.02199.
- Wei S, Nandi S, Chitu V, Yeung YG, Yu W, Huang M, et al. Functional overlap but differential expression of CSF-1 and IL-34 in their CSF-1 receptor-mediated regulation of myeloid cells. J Leukoc Biol. 2010;88(3):495–505. https://do i.org/10.1189/jlb.1209822.
- Freuchet A, Salama A, Remy S, Guillonneau C, Anegon I. IL-34 and CSF-1, Deciphering similarities and differences at steady state and in diseases. J Leukoc Biol. 2021;110(4):771–96. https://doi.org/10.1002/JLB.3RU1120-773R.
- Lelios I, Cansever D, Utz SG, Mildenberger W, Stifter SA, Greter M. Emerging roles of IL-34 in health and disease. J Exp Med. 2020;217(3). https://doi.org/10. 1084/jem.20190290.
- Belhocine S, Machado Xavier A, Distefano-Gagne F, Fiola S, Rivest S, Gosselin D. Context-dependent transcriptional regulation of microglial proliferation. Glia. 2022;70(3):572–89. https://doi.org/10.1002/glia.24124.
- Borst K, Schwabenland M, Prinz M. Microglia metabolism in health and disease. Neurochem Int. 2019;130:104331. https://doi.org/10.1016/j.neuint.20 18.11.006.
- Yamamoto S, Kohsaka S, Nakajima K. Role of cell cycle-associated proteins in microglial proliferation in the axotomized rat facial nucleus. Glia. 2012;60(4):570–81. https://doi.org/10.1002/glia.22291.
- Zhang Y, Li J, Zhao Y, Huang Y, Shi Z, Wang H, et al. Arresting the bad seed: HDAC3 regulates proliferation of different microglia after ischemic stroke. Sci Adv. 2024;10(10):eade6900. https://doi.org/10.1126/sciadv.ade6900.
- Wang Y, Szretter KJ, Vermi W, Gilfillan S, Rossini C, Cella M, et al. IL-34 is a tissue-restricted ligand of CSF1R required for the development of Langerhans cells and microglia. Nat Immunol. 2012;13(8):753–60. https://doi.org/10.1038/ ni.2360
- Emoto T, Lu J, Sivasubramaniyam T, Maan H, Khan AB, Abow AA, et al. Colony stimulating factor-1 producing endothelial cells and mesenchymal stromal cells maintain monocytes within a perivascular bone marrow niche. Immunity. 2022;55(5):862–e788. https://doi.org/10.1016/j.immuni.2022.04.005.
- Wang X, Zhao L, Zhang J, Fariss RN, Ma W, Kretschmer F, et al. Requirement for microglia for the maintenance of synaptic function and integrity in the mature retina. J Neurosci. 2016;36(9):2827–42. https://doi.org/10.1523/JNEUR OSCI.3575-15.2016.
- Guo C, Otani A, Oishi A, Kojima H, Makiyama Y, Nakagawa S, et al. Knockout of ccr2 alleviates photoreceptor cell death in a model of retinitis pigmentosa. Exp Eye Res. 2012;104:39–47. https://doi.org/10.1016/j.exer.2012.08.013.
- Hu Z, Zhang Y, Wang J, Mao P, Lv X, Yuan S, et al. Knockout of Ccr2 alleviates photoreceptor cell death in rodent retina exposed to chronic blue light. Cell Death Dis. 2016;7(11):e2468. https://doi.org/10.1038/cddis.2016.363.

- Li R, Zhang J, Wang Q, Cheng M, Lin B. TPM1 mediates inflammation downstream of TREM2 via the PKA/CREB signaling pathway. J Neuroinflammation. 2022;19(1):257. https://doi.org/10.1186/s12974-022-02619-3.
- Lehnardt S. Innate immunity and neuroinflammation in the CNS: the role of microglia in Toll-like receptor-mediated neuronal injury. Glia. 2010;58(3):253– 63. https://doi.org/10.1002/glia.20928.
- 67. Kaiser T, Feng G. Tmem119-EGFP and Tmem119-CreERT2 Transgenic mice for labeling and manipulating microglia. eNeuro. 2019;6(4). https://doi.org/10.15 23/ENEURO.0448-18.2019.
- Chen HR, Sun YY, Chen CW, Kuo YM, Kuan IS, Tiger Li ZR, et al. Fate mapping via CCR2-CreER mice reveals monocyte-to-microglia transition in development and neonatal stroke. Sci Adv. 2020;6(35):eabb2119. https://doi.org/10.1 126/sciadv.abb2119.
- Rowthorn-Apel N, Vridhachalam N, Connor KM, Bonilla GM, Sadreyev R, Singh C, et al. Microglial depletion decreases Muller cell maturation and inner retinal vascular density. Cell Commun Signal. 2025;23(1):90. https://doi.org/10 .1186/s12964-025-02083-5.
- 70. Claeys W, Verhaege D, Van Imschoot G, Van Wonterghem E, Van Acker L, Amelinck L, et al. Limitations of PLX3397 as a microglial investigational tool:

- peripheral and off-target effects dictate the response to inflammation. Front Immunol. 2023;14:1283711. https://doi.org/10.3389/fimmu.2023.1283711.
- Travor MD. Preclinical models of retinitis pigmentosa. Methods Mol Biol. 2023;2560:181–215. https://doi.org/10.1007/978-1-0716-2651-1\_19.
- 72. Guo Y, Wang P, Ma JH, Cui Z, Yu Q, Liu S, et al. Modeling retinitis pigmentosa: retinal organoids generated from the iPSCs of a patient with the USH2A mutation show early developmental abnormalities. Front Cell Neurosci. 2019;13:361. https://doi.org/10.3389/fncel.2019.00361.
- Ma C, Jin K, Jin ZB. Generation of human patient iPSC-derived retinal organoids to model retinitis pigmentosa. J Vis Exp. 2022(184). https://doi.org/10.37 91/64045

### Publisher's note

Springer Nature remains neutral with regard to jurisdictional claims in published maps and institutional affiliations.